Geological Magazine

www.cambridge.org/geo

Nature and origin of the volcanic ash beds near the Permian–Triassic boundary in South China: new data and their geological implications

Binsong Zheng[1,2,3,4], Chuanlong Mou[1,2,3,4,5], Renjie Zhou[6], Xiuping Wang[3,4], Zhaohui Xiao[7] and Yao Chen[7]

[1]School of Earth Sciences, China University of Geosciences, Wuhan 430074, China; [2]Chinese Academy of Geological Sciences, Beijing 100037, China; [3]Chengdu Institute of Geology and Mineral Resources, Chengdu 610081, China; [4]Key Laboratory for Sedimentary Basin and Oil and Gas Resources, Ministry of Natural Resources, Chengdu 610081, China; [5]College of Earth Science and Engineering, Shandong University of Science and Technology, Qingdao 266590, China; [6]School of Earth and Environmental Sciences, University of Queensland, St Lucia 4072, Australia and [7]Hubei Shale Gas Development Co. Ltd, Wuhan 430071, China

Original Article

Cite this article: Zheng B, Mou C, Zhou R, Wang X, Xiao Z, and Chen Y (2020) Nature and origin of the volcanic ash beds near the Permian–Triassic boundary in South China: new data and their geological implications. *Geological Magazine* **157**: 677–689. https://doi.org/10.1017/S001675681900133X

Received: 11 January 2019
Revised: 12 October 2019
Accepted: 15 October 2019
First published online: 3 December 2019

Keywords:
South China; western Hubei area; Permian–Triassic boundary volcanic ash bed; zircon; convergent continental margin

Author for correspondence:
Binsong Zheng and Chuanlong Mou,
Emails: michael199062@126.com and cdmchuanlong@163.com

Abstract

Permian–Triassic boundary (PTB) volcanic ash beds are widely distributed in South China and were proposed to have a connection with the PTB mass extinction and the assemblage of Pangea. However, their source and tectonic affinity have been highly debated. We present zircon U–Pb ages, trace-element and Hf isotopic data on three new-found PTB volcanic ash beds in the western Hubei area, South China. Laser ablation inductively coupled plasma mass spectrometry U–Pb dating of zircons yields ages of 252.2 ± 3.6 Ma, 251.6 ± 4.9 Ma and 250.4 ± 2.4 Ma for these three volcanic ash beds. Zircons of age *c.* 240–270 Ma zircons have negative $\varepsilon_{Hf}(t)$ values (–18.17 to –3.91) and Mesoproterozoic–Palaeoproterozoic two-stage Hf model ages (T_{Hf2}) (1.33–2.23 Ga). Integrated with other PTB ash beds in South China, zircon trace-element signatures and Hf isotopes indicate that they were likely sourced from intermediate to felsic volcanic centres along the Simao–Indochina convergent continental margin. The Qinling convergent continental margin might be another possible source but needs further investigation. Our data support the model that strong convergent margin volcanism took place around South China during late Permian – Early Triassic time, especially in the Simao–Indochina active continental margin and possibly the Qinling active continental margin. These volcanisms overlap temporally with the PTB biocrisis triggered by the Siberian Large Igneous Province. In addition, our data argue that the South China Craton and the Simao–Indochina block had not been amalgamated with the main body of Pangea by late Permian – Early Triassic time.

1. Introduction

Permian–Triassic boundary (PTB) volcanic ash beds are widely distributed in South China (Fig. 1). Their nature and origin have been studied for decades due to a possible relationship with the PTB mass extinction event and the assemblage of Pangea (e.g. Yin *et al.* 2007; Shen *et al.* 2011*a*; Burgess *et al.* 2014; Baresel *et al.* 2017). Petrographic and mineralogical studies demonstrate a felsic nature for these volcanic ash beds (He *et al.* 1989; Yin *et al.* 1989, 1992; Yang *et al.* 1991). The connection between the PTB mass extinction and the Siberian Large Igneous Province led to the conclusion that these ash beds may represent distal deposits from basaltic volcanisms of the Siberian Large Igneous Province (e.g. Shen *et al.* 2012). Studies on platinum-group elements in the PTB global stratotype section and point Meishan section also suggest a source from the Siberian Large Igneous Province and probably the Emeishan Large Igneous Province (Xu *et al.* 2007). Coeval tuffs found on the uppermost of the Emeishan basalt succession have led to the conclusion that these tuffs were sourced from the Emeishan Large Igneous Province (Zhu *et al.* 2011). However, recent studies (Yang *et al.* 2012; Gao *et al.* 2013, 2015; He *et al.* 2014) based on U–Pb ages, trace elements and Hf isotopes of zircons suggest that these volcanic ash beds may be sourced from convergent continental margins in the eastern Tethyan region, but precise locations are subject to debate. Existing studies argue for the convergent continental margin of the southwestern South China Craton (Yang *et al.* 2012; Gao *et al.* 2013, 2015) or the convergent continental margin in the East Kunlun area (He *et al.* 2014). In addition, these convergent events may have led to the amalgamation of East Asian blocks and Pangea (e.g. Metcalfe 1996, 2013; Huang *et al.* 2018; Zhao *et al.* 2018). The timing of the amalgamation is still under debate, however (e.g. Scotese & McKerrow, 1990; Collins, 2003; Scotese, 2004; Golonka *et al.* 2006; Golonka, 2007; Metcalfe, 2009;

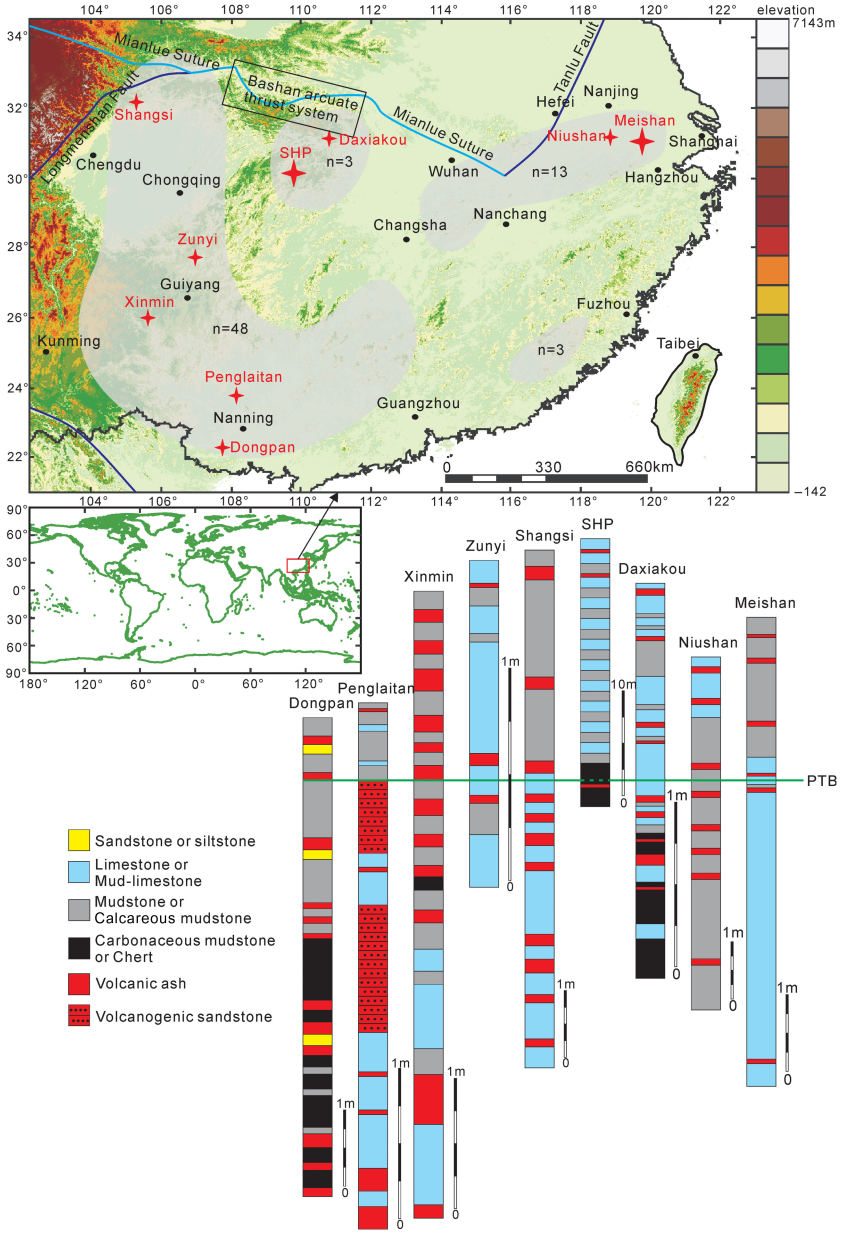

Fig. 1. (Color online) Distribution of PTB volcanic ash beds in South China (upper part) and correlation of representative PTB sections (lower part). The semitransparent areas in the upper map represent the distribution of volcanic ash beds, and *n* represents the number of sections. Volcanic ash bed localities and lithological columns are compiled from Yin *et al.* (1989), Yang *et al.* (1991, 2012), Shen *et al.* (2011*a*), Zhu *et al.* (2011), Gao *et al.* (2013, 2015), Burgess *et al.* (2014), He *et al.* (2014), Liao *et al.* (2016*a*, *b*), Baresel *et al.* (2017) and the SHP section in this study. Tectonic boundaries are from Zhang *et al.* (2004).

van der Meer *et al.* 2010; Cocks & Torsvik, 2013; Stampfli *et al.* 2013; Domeier & Torsvik, 2014; Huang *et al.* 2018; Zhao *et al.* 2018).

The PTB mass extinction was proposed to be triggered by Siberian Large Igneous Province flood basalt volcanism, which induced a world-wide lethally hot climate (e.g. Svensen *et al.* 2009; Joachimski *et al.* 2012; Sun *et al.* 2012; Retallack, 2013; Cui & Kump, 2015; Shen *et al.* 2016). Additionally, the timing of the PTB biocrisis and late Permian – Early Triassic convergent margin volcanism in the Palaeotethyan region has suggested that the Palaeotethys ignimbrite flare-up may also have contributed to the PTB mass extinction (e.g. Isozaki, 2009; Gao *et al.* 2013; He *et al.* 2014), but details of their relationship are still unclear.

In this study, we present data from three newly found PTB volcanic ash beds in the western Hubei area, South China, including zircon U–Pb ages, trace elements and Hf isotopes, and compare them with other PTB volcanic ash beds in South China. The source and tectonic affinity of these ashes are discussed. In addition, we also explore their possible relationship with the PTB mass extinction and the assemblage of Pangea.

2. Geological background

In South China, PTB volcanic ash beds, most of which have been diagenetically altered to clay beds, are widely distributed; up to 35 beds with a total thickness of up to 20 cm may be found in a single section (Fig. 1) (Yin *et al.* 1989; Yang *et al.* 1991; He *et al.* 2014). Their distinct color (e.g. white, yellow, light grey or greyish-green) and high content of clay minerals make them distinguishable from their surrounding rocks in the outcrop (Yang *et al.* 1991; Yin *et al.* 1992; Hong *et al.* 2008). Weighted mean ages of zircons from these ash beds range from 254.31 ± 0.07 Ma to 246.8 ± 1.3 Ma (Shen *et al.* 2011*a*; Zhu *et al.* 2011; Yang *et al.* 2012; Gao *et al.* 2013, 2015; Burgess *et al.* 2014; He *et al.* 2014; Liao *et al.* 2016*a*; Baresel *et al.* 2017).

https://doi.org/10.1017/S001675681900133X Published online by Cambridge University Press

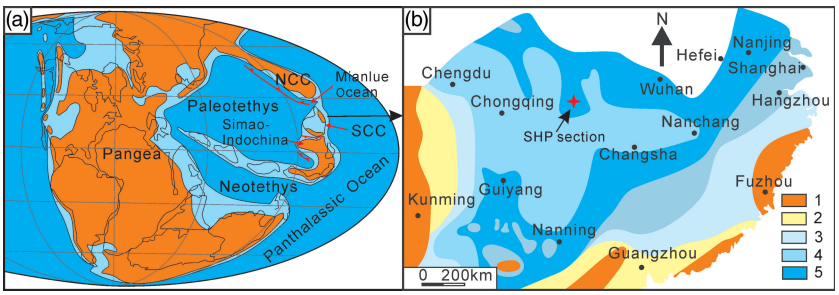

Fig. 2. (Color online) (a) Global palaeogeography at PTB (modified from Spörli *et al.* 2007). (b) Changhsingian palaeogeography of South China (modified from Feng *et al.* 1996*b*; Feng & Algeo, 2014). 1 – land; 2 – continental facies; 3 – littoral detrital facies; 4 – shallow-water carbonate; 5 –deep-water chert-mudstone; NCC – North China Craton; SCC – South China Craton; SHP – Shuanghe Poumian.

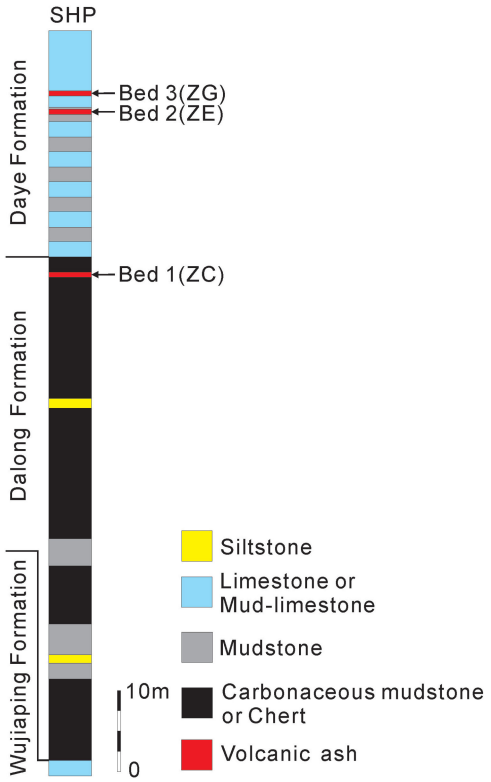

Fig. 3. (Color online) Lithologic column of the SHP section and sample locations.

The Shuanghe Poumian (SHP) section is located at the village of Shuanghe village, western Hubei area in the northern margin of South China Craton (30° 9′ 49.6″ N, 109° 48′ 6.4″ E). A continuous and well-exposed upper Permian – Lower Triassic deepwater succession has recently been identified (Figs 1, 2). The lower part of the SHP section is composed of the upper Permian Dalong Formation and the upper part is the Lower Triassic Daye Formation (Fig. 3). The Dalong Formation is *c.* 60 m thick and mainly composed of carbonaceous mudstone and chert with mudstone occasionally interbedded (Fig. 3). The lower part of the Daye Formation is approximately 25 m thick and mainly composed of interbedded limestone and mudstone (Fig. 3). The rest part of the Daye Formation is composed of limestone of approximately 800 m thickness. Biostratigraphy indicates a time range of late Wuchiapingian (late Permian) to Induan (Early Triassic), that is, *c.* 255–250 Ma (Gradstein *et al.* 2012), for the deposition of the Dalong Formation and the lower part of the Daye Formation (Fig. 4) (Zhang *et al.* 2009; Feng & Algeo, 2014; Zheng *et al.* 2019). Three PTB volcanic ash beds (beds 1 to 3) were studied (Figs 1, 3).

3. Samples and analytical methods

3.a. Sample description

Volcanic ash beds 1 to 3 were sampled and labelled as ZC, ZE and ZG, respectively (Fig. 3). These volcanic ash beds are 4–8 cm thick. They are distinct from their surrounding rocks in the outcrop due to their unique colour and high content of clay minerals similar to other sections in the adjacent area (Hong *et al.* 2008; Gao *et al.* 2013). Bed 1 is yellow to grey in colour and interbedded with carbonaceous mudstone at the top of the Dalong Formation. It contains millimetre-scale volcanic debris, indicating a proximal volcanic eruption (Fig. 5a, b). Beds 2 and 3 are grey-green in colour and interbedded with mudstone or limestone at the lower part of the Daye Formation (Fig. 5c, d).

3.b. Analytical methods

Zircon grains were separated using a combination of heavy liquid and magnetic separation techniques. Zircon grains were hand-picked and mounted in epoxy and polished. Zircon grains were imaged by a Gatan mini-cathodoluminescence (CL) spectroscope attached to a JSM6510 scanning electron microscope at Langfang Yuheng Mineral and Rock Service Ltd., Hebei, China, in order to reveal their internal structures.

U–Pb dating and trace-element analysis of zircons were conducted using laser ablation inductively coupled plasma mass spectrometry (LA-ICP-MS) at the Key Laboratory for the study of focused Magmatism and Giant Ore Deposits, Ministry of Natural Resources, in Xi'an Center of Geological Survey, China Geological Survey. Reference materials, 91500 and Plesovice zircons, and NIST610 glass were used. Laser ablation was performed using a GeoLas Pro laser-ablation system coupled to an Agilent 7700 × ICP-MS and the beam diameter was 24 μm. Each analysis incorporated a background acquisition of approximately 10 s (gas blank) followed by 40 s data acquisition. The Agilent Chemstation was utilized for the acquisition of each individual analysis. Off-line selection and integration of background and analytical signals, and time-drift correction and quantitative calibration for U–Pb dating, were performed using UranOS 2.06a (http://www.sediment.uni-goettingen.de/staff/dunkl/software) and trace-element analyses using Iolite 3.0 (http://iolite-software.com/). Weighted mean U–Pb ages (with 95% confidence) and concordia plots were generated by IsoPlot 3.75 (Ludwig, 2012). Grain ages use $^{207}Pb/^{206}Pb$ ages for grains older than 1.0 Ga and $^{206}Pb/^{238}U$ ages for younger grains.

In situ zircon Hf isotope analysis was performed using a GeoLas Pro laser-ablation system coupled to a Neptune multiple-collector ICP-MS at Xi'an Center of Geological Survey, China Geological Survey. Details of the instrumental conditions and data acquisition procedures are described by Meng *et al.* (2014). A beam diameter

https://doi.org/10.1017/S001675681900133X Published online by Cambridge University Press

Epoch	Stage	Formation	Ammonoid Zonation	Conodont zonation	Age (Ma)
Early Triassic	Induan	Daye	*Ophiceras-Hypophiceras-Lytophiceras*	*C.planata*	251
				I.isarcica-I.staeschei	
				H.parvus	252
Late Permian	Changhsingian	Dalong	*Pseudotirolites-Rotodiscoceras*	?	
				C.xiangsiensis-C.changxingensis	253
				C.postwangi-C.changxingensis	
			Sinoceltites	*C.subcarinata-C.wangi*	254
	Wuchiapingian		?	*C.orientalis*	
			Araxoceras-Konglingites-Sangyangites		255
		Wujiaping			

Fig. 4. The late Permian – Early Triassic succession of the study area (after Zhang *et al.* 2009; Zheng *et al.* 2019). The ages of the succession are from Gradstein *et al.* (2012).

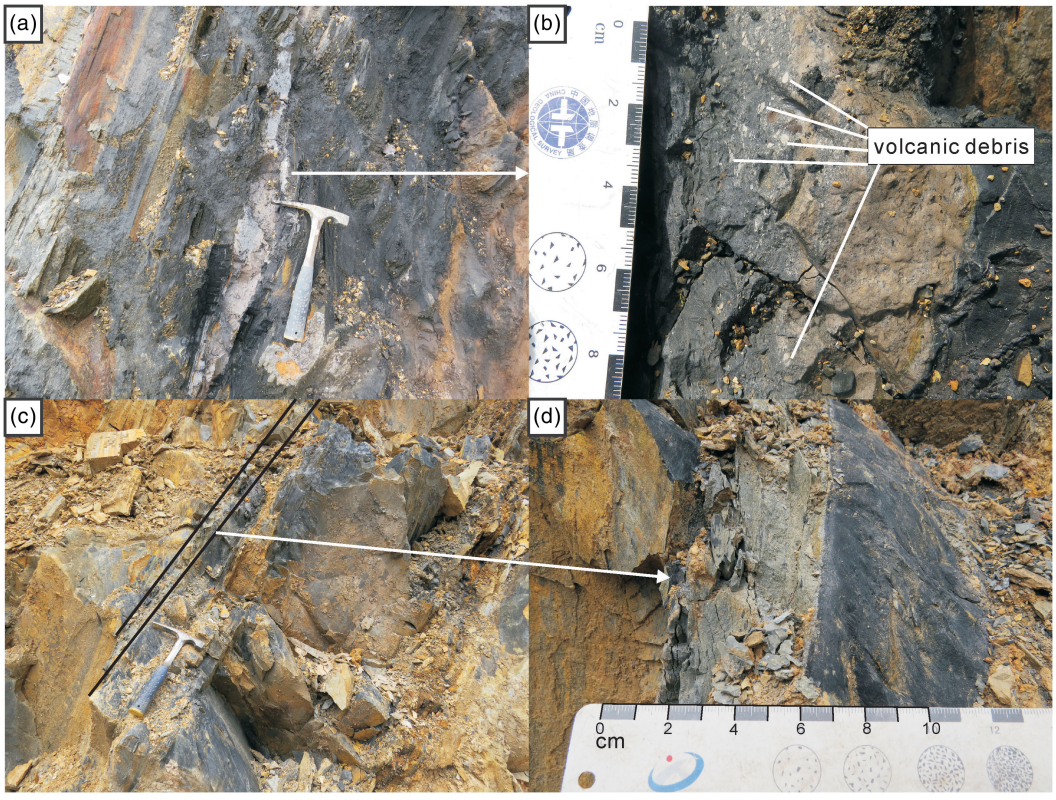

Fig. 5. (Color online) Outcrop photographs of the studied volcanic ash beds in the SHP section: (a, b) bed 1 (sample ZC) and (c, d) bed 3 (sample ZG).

https://doi.org/10.1017/S001675681900133X Published online by Cambridge University Press

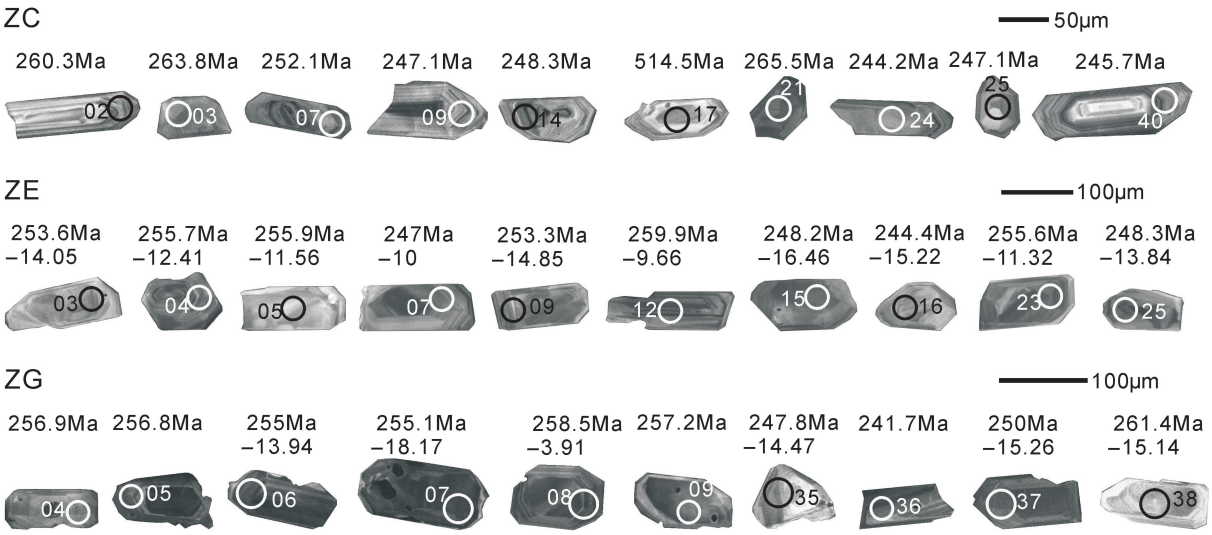

Fig. 6. Representative zircon CL images of our samples and their U–Pb ages and $\varepsilon_{Hf}(t)$ values. Circles represent laser pits.

of 32 μm was used on top of the existing laser pit for U–Pb for those zircons with large grain sizes. Correction factors for ^{176}Lu and ^{176}Yb isobaric interferences on ^{176}Hf are $^{176}Lu/^{175}Lu = 0.02658$ and $^{176}Yb/^{173}Yb = 0.796218$ (Chu *et al.* 2002). Instrumental mass bias was corrected by normalizing Yb isotope ratios to $^{172}Yb/^{173}Yb = 1.35274$ (Chu *et al.* 2002) and Hf isotopic ratios to $^{179}Hf/^{177}Hf = 0.7325$ using an exponential mass fractionation law. The mass bias behaviour of Lu was assumed to follow that of Yb. Details of the mass bias correction protocols are described in Iizuka & Hirata (2005), Wu *et al.* (2006) and Hou *et al.* (2007). Zircon GJ-1 was used as the reference standard and yielded a weighted mean $^{176}Hf/^{177}Hf$ ratio of 0.282030 ± 40 (2σ) for this study. This ratio overlaps with a weighted mean $^{176}Hf/^{177}Hf$ ratio of 0.282013 ± 19 (2σ) obtained by Elhlou *et al.* (2006). T_{Hf} and T_{Hf2} are single- and two-stage Hf model ages, respectively. The ε_{Hf}, T_{Hf} and $f_{Lu/Hf}$ in this study are calculated following Meng *et al.* (2014), where: the decay constant for ^{176}Lu is 1.867×10^{-11} a^{-1} (Amelin, 2005); $^{176}Lu/^{177}Hf$ and $^{176}Hf/^{177}Hf$ ratios for the chondritic reservoir are 0.0332 and 0.282772, respectively (Blichert-Toft & Albarede, 1997); $^{176}Lu/^{177}Hf$ and present-day $^{176}Hf/^{177}Hf$ ratios for the depleted mantle are 0.0384 and 0.28325, respectively (Griffin *et al.* 2000); and the $^{176}Lu/^{177}Hf$ ratio for average continental crust is 0.015 (Griffin *et al.* 2002).

4. Results

4.a. Zircon U–Pb ages

A total of 43 zircons from sample ZC (bed 1), 40 from sample ZE (bed 2) and 57 from sample ZG (bed 3) were dated (online Supplementary Table S1, available at http://journals.cambridge.org/geo). Analysed zircons are 60–200 μm prismatic euhedral crystals (Fig. 6), suggesting little transportation. Most of them have distinct oscillatory zoning, implying a magmatic origin (Fig. 6).

Among all zircons, 27 from ZC, 29 from ZE and 42 from ZG yield concordant U–Pb ages, and abundant ages fall near the PTB ranging from 237.2 ± 14.8 Ma to 271 ± 14.3 Ma ($n = 90$), which we used to calculate ages for the studied ash beds and obtained 252.2 ± 3.6 Ma (MSWD = 1.6) for Bed 1 (ZC), 251.6 ± 4.9 Ma (MSWD = 0.12) for Bed 2 (ZE) and 250.4 ± 2.4 Ma (MSWD = 0.46) for Bed 3 (ZG) (Supplementary Table S1; Fig. 7). Inherited zircon ages range from 444.8 ± 42.7 Ma to 2305.8 ± 60.4 Ma ($n = 8$) (Supplementary Table S1; Fig. 7).

4.b. Zircon trace elements

All zircons were analysed for their trace elements (online Supplementary Table S2, available at http://journals.cambridge.org/geo) and those with concordant U–Pb ages are summarized as follows. For all the samples, yttrium (Y) content ranges from 196 to 7340 ppm, hafnium (Hf) content ranges from 11090 to 18600 ppm and lead (Pb) content ranges from 11 to 735 ppm. The Th/U ratio ranges from 0.308 to 0.88 for sample ZC, 0.205–1.429 for sample ZE and 0.235–1.064 for sample ZG (Supplementary Table S1), indicating a magmatic origin (Rubatto, 2002). The chondrite-normalized rare Earth element (REE) pattern shows enrichment of heavy rare Earth elements (HREE), positive Ce anomaly and negative Eu anomaly, similar to other PTB volcanic ash beds in South China (Fig. 8).

4.c. Zircon Hf isotopes

Sixty zircon grains were analysed by *in situ* zircon Hf isotope analysis (online Supplementary Table S3, available at http://journals.cambridge.org/geo; Fig. 9a). $\varepsilon_{Hf}(t)$ values of the zircons aged *c.* 240–270 Ma range from −18.17 to −3.91, which is generally more negative than zircons from other volcanic ash beds in South China (Fig. 9b). Their T_{Hf} ages range from 0.84 to 1.46 Ga and T_{Hf2} ages range from 1.33 to 2.23 Ga. For inherited zircons, the $\varepsilon_{Hf}(t)$ values range from −50.98 to −9.59 with T_{Hf} ages of 1.05–2.73 Ga and T_{Hf2} ages of 1.69–4.23 Ga.

5. Discussion

5.a. Source and tectonic affinity of the volcanic ash beds

Trace elements may be diagnostic for source rocks and related tectonic backgrounds for magmatic zircons (Shnukov *et al.* 1997; Belousova *et al.* 2002; Grimes *et al.* 2007; Gao *et al.* 2013). Y versus U and Y versus $(Yb/Sm)_N$ plots show that zircons from PTB volcanic ash beds in the SHP section, as well as in

https://doi.org/10.1017/S001675681900133X Published online by Cambridge University Press

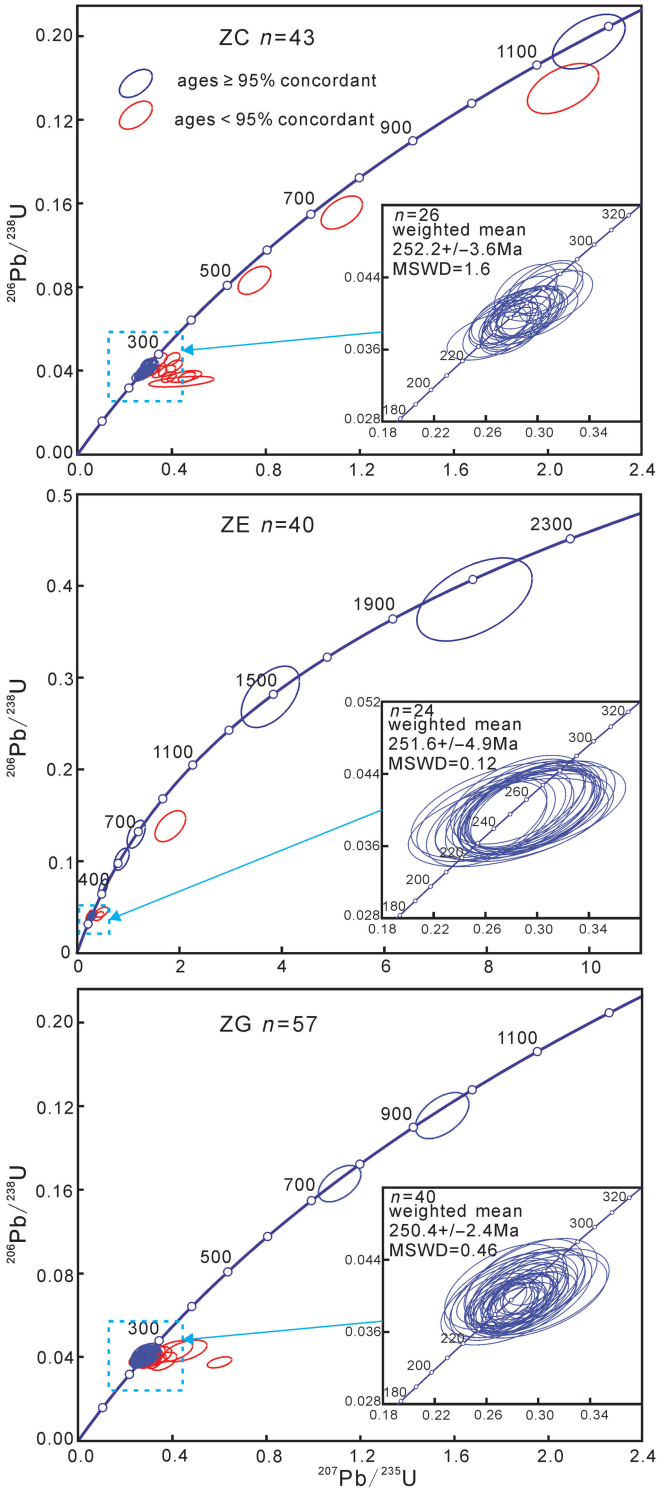

Fig. 7. (Color online) Zircon U–Pb concordia plots of samples (data-point error ellipses are 2σ).

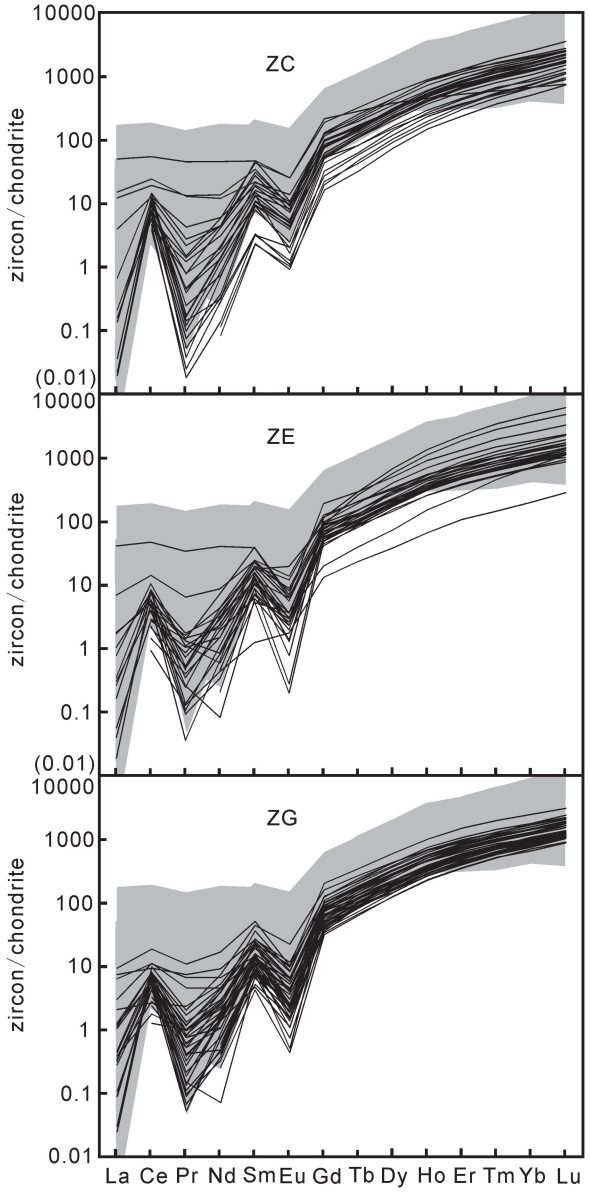

Fig. 8. Chondrite-normalized REE patterns for zircons. Chondritic values used for normalization are from Taylor & McLennan (1981). Curves represent zircons from the SHP section. Shaded areas are compiled from other PTB volcanic ash beds in South China (Yang *et al.* 2012; Gao *et al.* 2013, 2015).

other PTB sections in South China, were mainly distributed in the areas of felsic rocks, such as granitoids, larvikites and syenite pegmatites, and the area of mafic rocks that overlaps with felsic rocks (Fig. 10a, b). The Y versus Hf plot points to an intermediate to felsic source (Fig. 10c). The Y versus (U/Yb) diagram shows that these zircons were most likely sourced from felsic volcanic sources at convergent continental margins before post-collisional extension (Fig. 10d).

The values of $\varepsilon_{Hf}(t)$ and T_{Hf2} ages of the zircons aged *c.* 240–270 Ma in the SHP section as well as in other PTB sections in South China indicate that the parent magma might be mainly sourced from Palaeoproterozoic–Mesoproterozoic crustal materials (online Supplementary Table S3, available at http://journals.cambridge.org/geo; Figs 9, 11). However, pre-Palaeoproterozoic T_{Hf2} ages from ancient zircon cores (Figs 9, 11) provide a possibility that the source of magma may require some contribution from younger (post-Mesoproterozoic) juvenile materials. Slightly positive to slightly negative $\varepsilon_{Hf}(t)$ values in some sections also imply a contribution from juvenile mantle-derived mafic materials to the source magma (Fig. 9b) (e.g. Gao *et al.* 2013).

In summary, PTB volcanic ash beds in South China may be sourced from intermediate to felsic volcanisms at convergent continental margins before post-collisional extension. Their source magma may have been mainly derived from

https://doi.org/10.1017/S001675681900133X Published online by Cambridge University Press

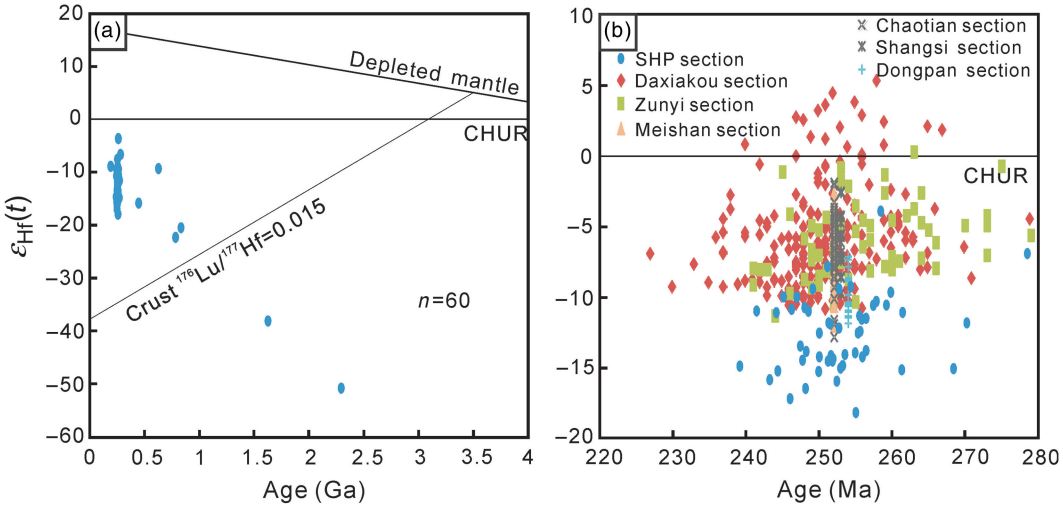

Fig. 9. (Color online) $\varepsilon_{Hf}(t)$ plots for zircons: (a) from the SHP section; and (b) of age *c.* 240–270 Ma different PTB sections in South China. Daxiakou section is from Gao *et al.* (2013), Zunyi section is from Gao *et al.* (2015), Meishan section, Chaotian section, Shangsi section and Dongpan section are from He *et al.* (2014).

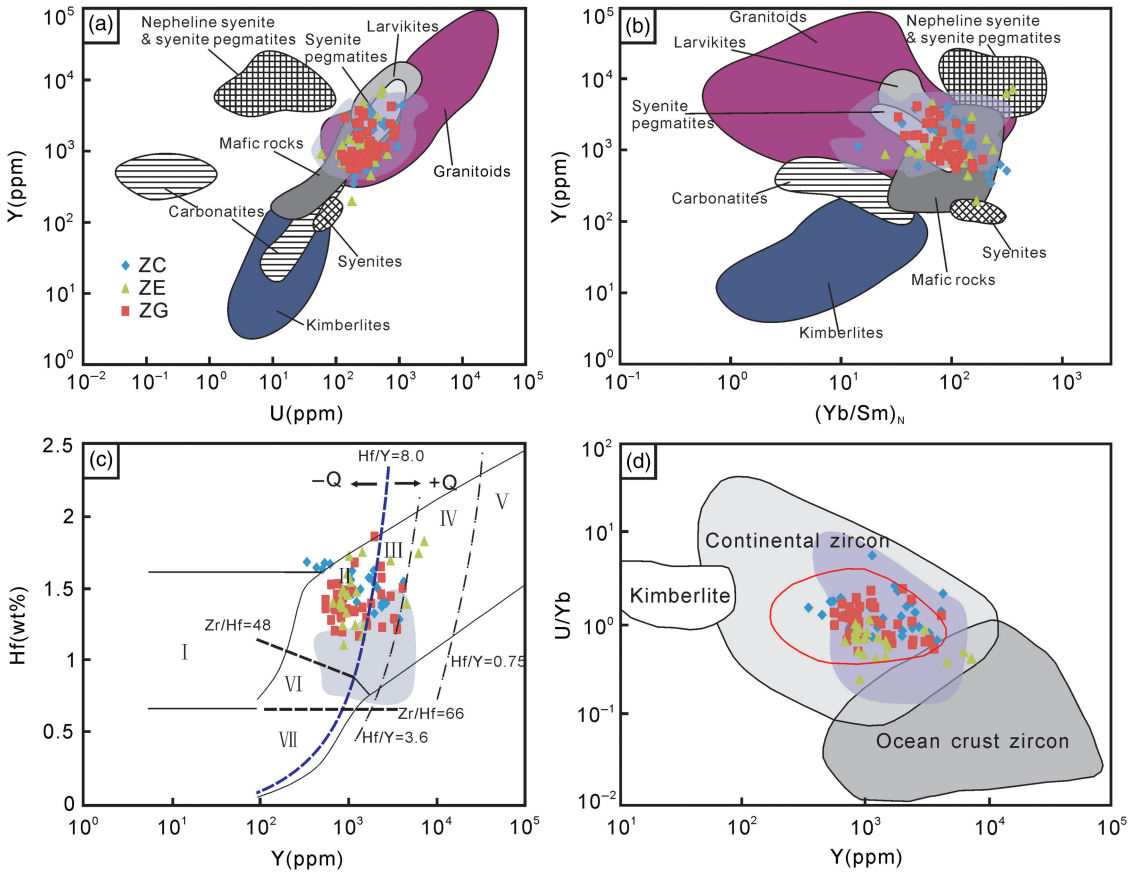

Fig. 10. (Color online) Trace-element diagrams for source rock and tectonic setting discrimination of the zircons aged *c.* 240–270 Ma. (a–c) Y versus U, Y versus $(Yb/Sm)_N$ and Hf versus Y diagrams for source-rock discrimination (Shnukov *et al.* 1997; Belousova *et al.* 2002), where subscript N represents chondrite-normalized value; I – kimberlites; II – ultramafic, mafic and intermediate rocks; III – quartz-bearing intermediate and felsic rocks; IV – felsic rocks with high SiO_2 content; V – greisens; VI – alkaline rocks and alkaline metasomatites of alkaline complexes; VII – carbonatites. (d) U/Yb versus Y diagram for tectonic setting discrimination (Grimes *et al.* 2007; Gao *et al.* 2013). The red circle represents zircons from felsic rocks at convergent continental margins before post-collisional extension. The shaded area represents data compiled from other PTB volcanic ash beds in South China (after Yang *et al.* 2012; Gao *et al.* 2013, 2015).

Palaeoproterozoic–Mesoproterozoic crustal materials with juvenile mantle-derived mafic materials contributing to varying degrees.

5.b. Location of the volcanic source

Two theories exist for the source of PTB volcanic ash beds in South China. A first view suggests that these volcanic ash beds may be sourced from the Siberian Large Igneous Province and probably the Emeishan Large Igneous Province (e.g. Xu *et al.* 2007; Zhu *et al.* 2011; Shen *et al.* 2012). For the Siberian Large Igneous Province, the maximum age for pyroclastic magmatism was dated at 255.58 ± 0.38 Ma and the youngest felsic tuff bed was dated at 251.403 ± 0.048 Ma (Burgess & Bowring, 2015), indicating an overlap in timing with those coeval volcanic ash beds in South

https://doi.org/10.1017/S001675681900133X Published online by Cambridge University Press

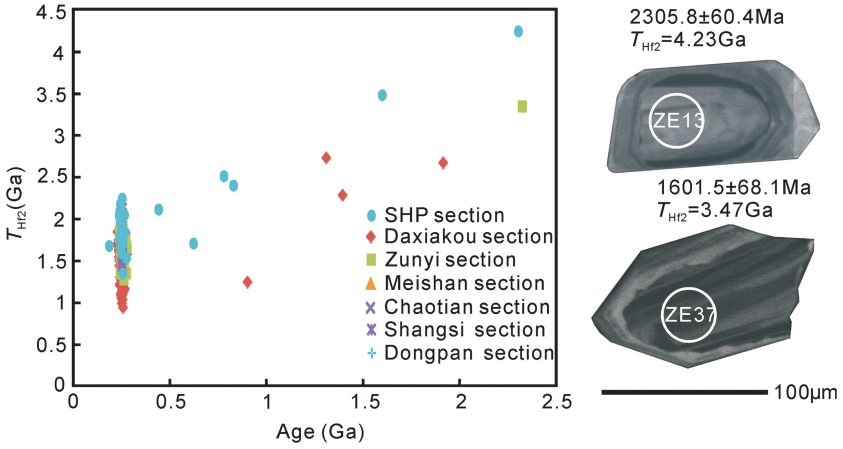

Fig. 11. (Color online) T_{Hf2} ages of zircons from different PTB volcanic ash beds in South China. Daxiakou section is from Gao *et al.* (2013), Zunyi section is from Gao *et al.* (2015), and Meishan, Chaotian, Shangsi and Dongpan sections are from He *et al.* (2014).

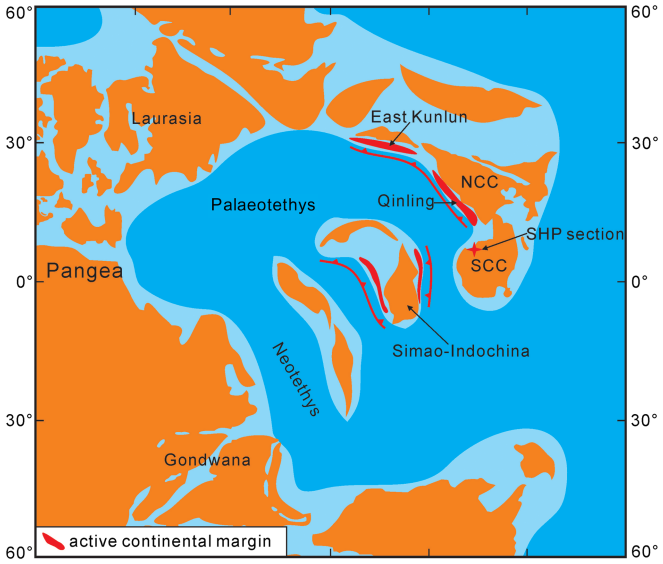

Fig. 12. (Color online) Late Permian palaeogeography map of the Palaeotethys region showing the convergent continental margins around South China (modified from Huang *et al.* 2018). Detailed palaeogeography of South China Craton is shown in Figure 2b.

China except for those later during Early Triassic time. For the Emeishan Large Igneous Province in southwestern South China, the major basaltic eruption is thought to have occurred at *c.* 260 Ma (He *et al.* 2003) and the associated intermediate to felsic plutons were dated at *c.* 260–251 Ma (Xu *et al.* 2008; Shellnutt *et al.* 2009; Zhong *et al.* 2009, 2011; He, 2016), regardless of the compositional discrepancy, also suggesting a timing overlap with those coeval volcanic ash beds in South China except for those later during Early Triassic time. A second view argues that they may have been sourced from intermediate to felsic volcanism that is related to the closure of the Palaeotethys Ocean or the formation of the Pangea supercontinent (Clark *et al.* 1986; He *et al.* 1989, 2014; Yin *et al.* 1989, 1992, 2007; Yang *et al.* 1991, 2012; Isozaki *et al.* 2007; Gao *et al.* 2013, 2015).

Our data argue for a convergent continental margin source for the PTB ash beds in South China; however, the precise location of the source volcanism is subject to debate. Existing studies argue for the convergent continental margin of the southwestern South China Craton (Yang *et al.* 2012; Gao *et al.* 2013, 2015) or the convergent continental margin in the East Kunlun area (He *et al.* 2014). However, except for the intermediate to felsic nature and their tectonic affinity to magmatic arc, the link between these possible parent volcanisms and PTB volcanic ash beds in South China was mainly developed based on obtained ages and the spatial variation in the thickness and numbers of the PTB ash beds.

During late Permian – Early Triassic time, the subduction of the Palaeotethys Ocean resulted in the formation of several convergent continental margins in the eastern Palaeotethys region (Huang *et al.* 2018), including the Kunlun (e.g. Xiao *et al.* 2002; Yan *et al.* 2008; Dai *et al.* 2013), Qinling (e.g. Guo *et al.* 2012; Yan *et al.* 2012, 2014; Dong & Santosh, 2016) and Simao–Indochina convergent continental margins (e.g. Cai & Zhang, 2009; Faure *et al.* 2014; Liu *et al.* 2018) (Fig. 12). These coeval convergent continental margins are the most likely sources for PTB ash beds in South China. Zircon Hf isotopes and model ages are useful indicators of tectonic setting and the nature of the associated magma, providing a possibility to precisely locate the parent volcanism of PTB ash beds in South China. Available data allow us to directly compare these Hf-related parameters of magmatic zircons in PTB ash beds in South China with those in coeval intermediate to felsic magmatic rocks (*c.* 255–246 Ma) in Simao–Indochina and East Kunlun convergent continental margins. For

https://doi.org/10.1017/S001675681900133X Published online by Cambridge University Press

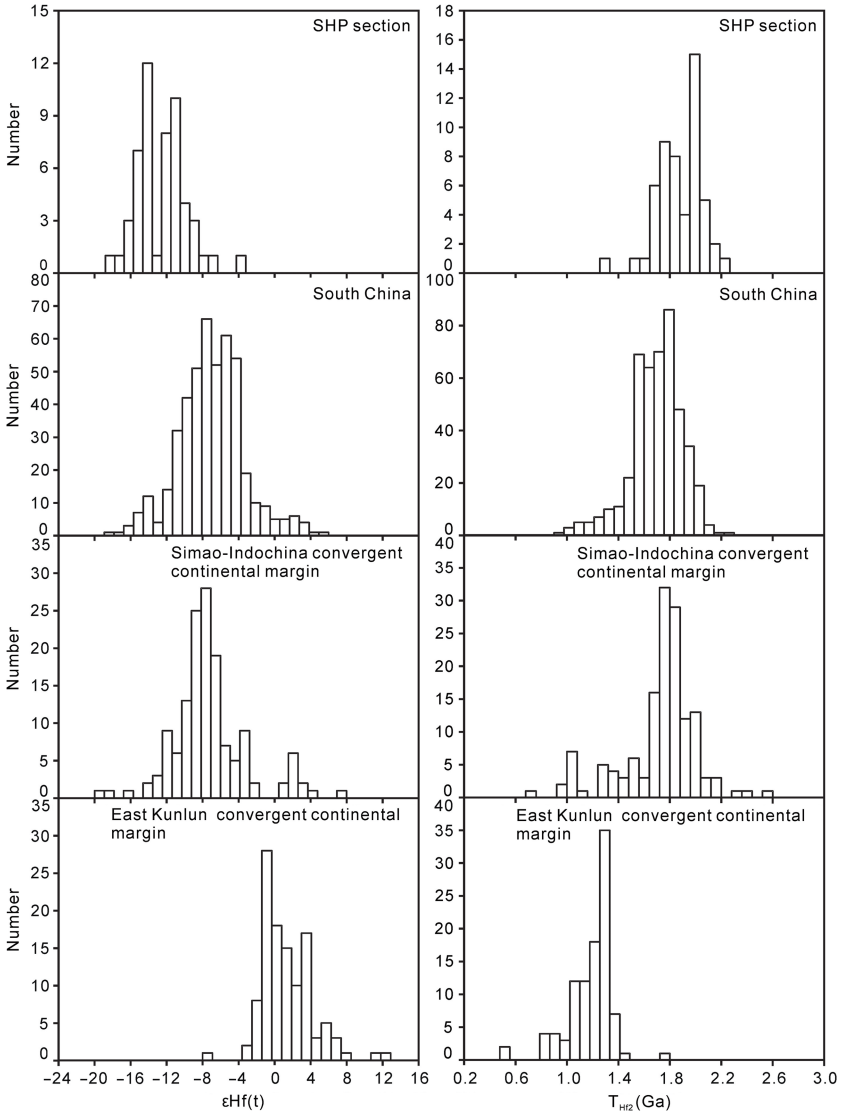

Fig. 13. Zircon $\varepsilon_{Hf}(t)$ value and T_{Hf2} age histograms of PTB ash beds in South China and late Permian – Early Triassic intermediate to felsic magmatic rocks in Simao–Indochina and East Kunlun convergent continental margins. Data for South China PTB ash beds are compiled from Gao *et al.* (2013, 2015) and He *et al.* (2014). Data for Simao–Indochina convergent continental margin are compiled from Zi *et al.* (2012), Li *et al.* (2013) and Liu *et al.* (2015). Data for East Kunlun convergent continental margin are compiled from Huang *et al.* (2014), Ding *et al.* (2015) and Ren *et al.* (2016).

the coeval magmatic zircons in the Simao–Indochina convergent continental margin, both $\varepsilon_{Hf}(t)$ values and T_{Hf2} ages overlap those in PTB ash beds in South China, and their distribution patterns also show similarities with $\varepsilon_{Hf}(t)$ values of *c.* −12 to −4 and T_{Hf2} ages of *c.* 1.5–2.1 Ga (Fig. 13), indicating that the Simao–Indochina convergent continental margin may be the major source of PTB ash beds in South China. The coeval magmatic zircons in the East Kunlun convergent continental margin generally show higher $\varepsilon_{Hf}(t)$ values and younger T_{Hf2} ages compared with those in PTB ash beds in South China (Fig. 13), indicating the East Kunlun convergent continental margin is unlikely to be the major source. For the Qinling convergent continental margin, metamorphic ages of the subducted oceanic crust (Sun *et al.* 2002; Cheng *et al.* 2009; Wu *et al.* 2009; Liu *et al.* 2011) and ages of arc-related volcanic rocks (Feng *et al.* 1996*a*; Li *et al.* 2004) indicate that the subduction of the oceanic crust under the Qinling – North China composite continent occurred during Carboniferous time. Palaeomagnetic data (Zhao & Coe, 1987; Enkin *et al.* 1992; Yang *et al.* 1998; Zhu *et al.* 1998; Huang *et al.* 2018) and high and ultrahigh-pressure eclogite facies metamorphic events in the Dabie mountains (Liu *et al.* 2008; Cheng *et al.* 2011; Gao *et al.* 2011; Liu & Liou, 2011) support a scissors-like closure of the ocean between South and North China cratons that was initiated during Late Permian time, with its eastern part closed earlier. The final collision in the western orogen occurred during late Triassic time as evidenced by a large volume of collision-related granitoids in the western Qinling area (Wang *et al.* 2015). However, the suture zone has been intensely reworked by the Mesozoic and Cenozoic intracontinental orogeny and mostly covered by the Bashan arcuate thrust system (Zhang *et al.* 2004), and the late Permian – Early Triassic intermediate to felsic magmatic rocks have not yet been found. However, as an adjacent coeval active continental margin (Fig. 12), it cannot be excluded as a possible source for the PTB ash beds in South China. Considering the large number of PTB ash beds and their wide distribution in South China (Fig. 1), they may not be derived from a single source. For example, magmatic zircons in the SHP section, adjacent to the Qinling convergent continental margin (Fig. 12), generally show lower $\varepsilon_{Hf}(t)$ values and older T_{Hf2} ages compared with those in other PTB ash beds in South China (Fig. 13), providing the possibility that they may be sourced from the Qinling convergent continental margin.

https://doi.org/10.1017/S001675681900133X Published online by Cambridge University Press

5.c. Geological implications

The *c.* 252 Ma PTB mass extinction caused a reduction of *c.* 70% of terrestrial and *c.* 90% of marine species and the ecosystem took 5 Ma or longer to recover from the extinction (Chen *et al.* 2014; Algeo *et al.* 2015). The Siberian Large Igneous Province flood basalt volcanism was proposed to trigger the PTB mass extinction by inducing the lethally hot climate (Wignall, 2001; Retallack & Jahren, 2008; Svensen *et al.* 2009; Joachimski *et al.* 2012; Shen *et al.* 2012, 2013, 2016; Sun *et al.* 2012; Retallack, 2013; Cui & Kump, 2015). In addition, Isozaki (2009) and He *et al.* (2014) proposed that possible Palaeotethys ignimbrite flare-up may have injected a large volume of sulphur aerosols and ash particles into the late Permian – Early Triassic stratosphere, which may have caused severe environmental changes in the biosphere in a 'volcanic ash winter' scenario. Shen *et al.* (2011*b*) and Gao *et al.* (2013) proposed that, as a plausible heat source, silicic volcanism at a convergent continental margin related to Palaeotethys subduction may also have triggered the widespread wildfires on the continent, evidenced by combustion-derived black carbon and polynuclear aromatic hydrocarbons found in sediments in the PTB global stratotype section and point Meishan section. Our data reveal that the long-term intermediate to felsic volcanism at convergent continental margins around South China overlap temporally with the PTB biocrisis triggered by the Siberian Large Igneous Province flood basalt volcanism.

Pangea formed at *c.* 320–250 Ma with Laurasia in the north and Gondwana in the south (Fig. 12) (Smith & Livermore, 1991; Murphy & Nance, 2008; Stampfli *et al.* 2013). However, it is controversial whether East Asian blocks have ever been a part of Pangea before it broke up during Early Jurassic time (e.g. Scotese & McKerrow, 1990; Collins, 2003; Scotese, 2004; Golonka *et al.* 2006; Golonka, 2007; Metcalfe, 2009; van der Meer *et al.* 2010; Cocks & Torsvik, 2013; Stampfli *et al.* 2013; Domeier & Torsvik, 2014; Huang *et al.* 2018; Zhao *et al.* 2018). Regarding the South China Craton and the Simao–Indochina block, most reconstructions propose that they may have been separated from Pangea by the Palaeotethys Ocean (e.g. Collins, 2003; Scotese, 2004; Golonka, 2007; Metcalfe, 2009; Cocks & Torsvik, 2013; Domeier & Torsvik, 2014). Recent studies on palaeomagnetism and orogenic belts of East Asian blocks argue that these two blocks may have been connected to Pangea by *c.* 220 Ma (Huang *et al.* 2018; Zhao *et al.* 2018). Our data support the theory that strong magmatic activity may have taken place in the Simao–Indochina active continental margin and possibly the Qinling active continental margin of North China Craton during late Permian – Early Triassic time, indicating that eastern branches of the Palaeotethys Ocean, which separated the South China Craton and Simao–Indochina block from Pangea, had not yet been completely consumed during this time (Fig. 12).

6. Conclusions

Three volcanic ash beds (beds 1 to 3) were reported in the late Permian – Early Triassic SHP section in the western Hubei area, South China. LA–ICP–MS U–Pb dating of zircons yields ages of 252.2 ± 3.6 Ma for bed 1, 251.6 ± 4.9 Ma for bed 2 and 250.4 ± 2.4 Ma for bed 3. Zircon trace-element signatures and Hf isotopes indicate that the PTB volcanic ash beds in South China were likely sourced from coeval intermediate to felsic volcanic sources at the Simao–Indochina convergent continental margin. The Qinling active continental margin may be another source, but this possibility requires further investigation before being considered seriously.

Our new data indicate that convergent continental margin magmatism took place around South China during late Permian – Early Triassic time, especially in the Simao–Indochina active continental margin and possibly the Qinling active continental margin. These volcanisms took place around the same time as the PTB biocrisis triggered by the Siberian Large Igneous Province. In addition, our data indicate that the South China Craton and Simao–Indochina block had not been amalgamated with Pangea by late Permian – Early Triassic time.

Acknowledgments. This work was supported by the Shale Gas Development Co. Ltd, Hubei Province, China (contract no. HBYYQ-GC1075) and the National Natural Science Foundation of China (project no. 41772113). Binsong Zheng was supported by the Joint Training study program for excellent doctoral candidates at the School of Earth Sciences, China University of Geosciences (Wuhan). We would also like to thank the editor and the reviewers for their constructive comments and suggestions.

Supplementary material. To view supplementary material for this article, please visit https://doi.org/10.1017/S001675681900133X.

References

Algeo TJ, Chen ZQ and Bottjer DJ (2015) Global review of the Permian–Triassic mass extinction and subsequent recovery: part II. *Earth-Science Reviews* **149**, 1–4.

Amelin Y (2005) Meteorite phosphates show constant ^{176}Lu decay rate since 4557 million years ago. *Science* **310**, 839–41.

Baresel B, Bucher H, Brosse M, Cordey F, Guodun K and Schaltegger U (2017) Precise age for the Permian–Triassic boundary in South China from high-precision U-Pb geochronology and Bayesian age–depth modeling. *Solid Earth* **8**, 361–78.

Belousova EA, Griffin WL, O'Reilly SY and Fisher NI (2002) Igneous zircon: trace element composition as an indicator of source rock type. *Contributions to Mineralogy and Petrology* **143**, 602–22.

Blichert-Toft J and Albarede F (1997) The Lu–Hf isotope geochemistry of chondrites and the evolution of the mantle-crust system. *Earth and Planetary Science Letters* **148**, 243–58.

Burgess SD and Bowring SA (2015) High-precision geochronology confirms voluminous magmatism before, during, and after Earth's most severe extinction. *Science Advances* **1**, 1–14.

Burgess SD, Bowring SA and Shen SZ (2014) High-precision timeline for Earth's most severe extinction. *Proceedings of the National Academy of Sciences* **111**, 3316–21.

Cai J-X and Zhang K-J (2009) A new model for the Indochina and South China collision during the Late Permian to the Middle Triassic. *Tectonophysics* **467**, 35–43.

Chen ZQ, Algeo TJ and Bottjer DJ (2014) Global review of the Permian–Triassic mass extinction and subsequent recovery: part I. *Earth-Science Reviews* **137**, 1–5.

Cheng H, King RL, Nakamura E, Vervoort JD, Zheng YF, Ota T, Wu YB, Kobayashi K and Zhou ZY (2009) Transitional time of oceanic to continental subduction in the Dabie orogen: constraints from U-Pb, Lu-Hf, Sm-Nd and Ar-Ar multichronometric dating. *Lithos* **110**, 327–42.

Cheng H, Zhang C, Vervoort JD, Wu YB, Zheng YF, Zheng S and Zhou ZY (2011) New Lu–Hf geochronology constrains the onset of continental subduction in the Dabie orogen. *Lithos* **121**, 41–54.

Chu NC, Taylor RN, Chavagnac V, Nesbitt RW, Boella RM, Milton JA, German CR, Bayon G and Burton K (2002) Hf isotope ratio analysis using multi-collector inductively coupled plasma mass spectrometry: an evaluation of isobaric interference corrections. *Journal of Analytical Atomic Spectrometry* **17**, 1567–74.

Clark DL, Wang CY, Orth CJ and Gilmore JS (1986) Conodont survival and low iridium abundances across the Permian–Triassic boundary in South-China. *Science* **233**, 984–6.

Cocks LRM and Torsvik TH (2013) The dynamic evolution of the Palaeozoic geography of eastern Asia. *Earth-Science Reviews* **117**, 40–79.

Collins WJ (2003) Slab pull, mantle convection, and Pangaean assembly and dispersal. *Earth and Planetary Science Letters* **205**, 225–37.

Cui Y and Kump LR (2015) Global warming and the end-Permian extinction event: Proxy and modeling perspectives. *Earth-Science Reviews* **149**, 5–22.

Dai JG, Wang CS, Hourigan J and Santosh M (2013) Multi-stage tectono-magmatic events of the Eastern Kunlun Range, northern Tibet: Insights from U–Pb geochronology and (U–Th)/He thermochronology. *Tectonophysics* **599**, 97–106.

Ding QF, Liu F and Yan W (2015) Zircon U–Pb geochronology and Hf isotopic constraints on the petrogenesis of Early Triassic granites in the Wulonggou area of the Eastern Kunlun Orogen, Northwest China. *International Geology Review* **57**, 1735–54.

Domeier M and Torsvik TH (2014) Plate tectonics in the late Paleozoic. *Geoscience Frontiers* **5**, 303–50.

Dong YP and Santosh M (2016) Tectonic architecture and multiple orogeny of the Qinling Orogenic Belt, Central China. *Gondwana Research* **29**, 1–40.

Elhlou S, Belousova E, Griffin WL, Pearson NJ and O'Reilly SY (2006) Trace element and isotopic composition of GJ-red zircon standard by laser ablation. *Geochimica et Cosmochimica Acta* **70**, A158.

Enkin RJ, Yang Z, Chen Y and Courtillot V (1992) Paleomagnetic constraints on the geodynamic history of the major blocks of China from Permian to the present. *Journal of Geophysical Research* **97**, 13953–89.

Faure M, Lepvrier C, Nguyen VV, Vu TV, Lin W and Chen Z (2014) The South China block-Indochina collision: Where, when, and how? *Journal of Asian Earth Sciences* **79**, 260–74.

Feng QL and Algeo TJ (2014) Evolution of oceanic redox conditions during the Permo–Triassic transition: evidence from deepwater radiolarian facies. *Earth-Science Reviews* **137**, 34–51.

Feng ZZ, Yang YQ, Jin ZK, He YB, Wu SH, Xin WJ, Bao ZD and Tan J (1996b) Lithofacies paleogeography of the Permian of South China. *Acta Sedimentologica Sinica* **14**, 1–11 (in Chinese with English abstract).

Feng QL, Du YS, Yin HF, Sheng JH and Xu JF (1996a) Carboniferous radiolaria fauna firstly discovered in Mian-Lüe ophiolitic mélange belt of South Qinling Mountains. *Science in China (Series D)* **39**, 87–92.

Gao Q, Chen ZQ, Zhang N, Griffin WL, Xia W, Wang G, Jiang T, Xia X and O'Reilly SY (2015) Ages, trace elements and Hf-isotopic compositions of zircons from claystones around the Permian–Triassic boundary in the Zunyi Section, South China: implications for nature and tectonic setting of the volcanism. *Journal of Earth Science* **26**, 872–82.

Gao Q, Zhang N, Xia W, Feng Q, Chen ZQ, Zheng J, Griffin WL, O'Reilly SY, Pearson NJ, Wang G, Wu S, Zhong W and Sun X (2013) Origin of volcanic ash beds across the Permian–Triassic boundary, Daxiakou, South China: petrology and U-Pb age, trace elements and Hf-isotope composition of zircon. *Chemical Geology* **360–361**, 41–53.

Gao XY, Zheng YF and Chen YX (2011) U-Pb ages and trace elements in metamorphic zircon and titanite from UHP eclogite in the Dabie orogen: constraints on P–T–t path. *Journal of Metamorphic Geology* **29**, 721–40.

Golonka J (2007) Late Triassic and Early Jurassic palaeogeography of the world. *Palaeogeography, Palaeoclimatology, Palaeoecology* **244**, 297–307.

Golonka J, Krobicki M, Pająk J, Nguyen VG and Zuchiewicz W (2006) *Global Plate Tectonics and Paleogeography of Southeast Asia*. Faculty of Geology, Geophysics and Environmental Protection, AGH University of Science and Technology, 128 pp.

Gradstein FM, Ogg JG, Schmitz MD and Ogg G (2012) *The Geologic Time Scale 2012*. Amsterdam: Elsevier, 1176 pp.

Griffin WL, Pearson NJ, Belousova EA, Jackson SE, van Achterbergh E, O'Reilly SY and Shee SR (2000) The Hf isotope composition of cratonic mantle: LA-MC-ICPMS analysis of zircon megacrysts in kimberlites. *Geochimica et Cosmochimica Acta* **64**, 133–47.

Griffin WL, Wang X, Jackson SE, Pearson NJ and O'Reilly SY (2002) Zircon chemistry and magma mixing, SE China: in-situ analysis of Hf isotopes, Tonglu and Pingtan igneous complexes. *Lithos* **61**, 237–69.

Grimes CB, John BE, Kelermen PB, Mazdab FK, Wooden JL, Cheadle MJ, Hanghoj K and Schwartz JJ (2007) Trace element chemistry of zircons from oceanic crust: a method for distinguishing detrital zircon provenance. *Geology* **35**, 643–6.

Guo X, Yan Z, Wang Z, Wang T, Hou K, Fu C and Li J (2012) Middle-Triassic arc magmatism along the northeastern margin of the Tibet: U-Pb and Lu-Hf zircon characterization of the Gangcha complex in the West Qinling terrane, central China. *Journal of Geological Society, London* **169**, 327–36.

He B, Xu Y, Chung SL, Xiao L and Wang Y (2003) Sedimentary evidence for a rapid, kilometer-scale crustal doming prior to the eruption of the Emeishan flood basalts. *Earth and Planetary Science Letters* **213**, 391–405.

He B, Zhong YT, Xu YG and Li XH (2014) Triggers of Permo-Triassic boundary mass extinction in South China: The Siberian Traps or Paleo-Tethys ignimbrite flare-up? *Lithos* **204**, 258–67.

He BH (2016) Research progress on some issues on the Emeishan Large Igneous Province. *Advances in Earth Science* **31**, 23–42 (in Chinese with English abstract).

He JW, Chai ZF and Ma SL (1989) Discovery of paramorph of high-quartz in the stratotype section of the Permian–Triassic boundary at Meishan of Changxing, Zhejiang, and its significance. *Chinese Science Bulletin* **34**, 474–7.

Hong HL, Zhang N, Li ZH, Xue HJ, Xia WC and Yu N (2008) Clay mineralogy across the P–T boundary of the Xiakou section, China: evidence of clay provenance and environment. *Clays and Clay Minerals* **56**, 131–43.

Hou KJ, Li YH, Zou TR, Qu XM, Shi YR and Xie GQ (2007) Laser ablation-MC-ICP-MS technique for Hf isotope microanalysis of zircon and its geological applications. *Acta Petrologica Sinica* **23**, 2595–604 (in Chinese with English abstract).

Huang BC, Yan YG, Piper JDA, Zhang DH, Yi ZY, Yu S and Zhou TH (2018) Paleomagnetic constraints on the paleogeography of the East Asian blocks during Late Paleozoic and Early Mesozoic times. *Earth-Science Reviews* **186**, 8–36.

Huang H, Niu YL, Nowell G, Zhao ZD, Yu XH, Zhu DC, Mo XX and Ding S (2014) Geochemical constraints on the petrogenesis of granitoids in the East Kunlun Orogenic belt, northern Tibetan Plateau: implications for continental crust growth through syn-collisional felsic magmatism. *Chemical Geology* **370**, 1–18.

Iizuka T and Hirata T (2005) Improvements of precision and accuracy in in situ Hf isotope microanalysis of zircon using the laser ablation-MC-ICPMS technique. *Chemical Geology* **220**, 121–37.

Isozaki Y (2009) Integrated "plume winter" scenario for the double-phased extinction during the Paleozoic-Mesozoic transition: The G-LB and P-TB events from a Panthalassan perspective. *Journal of Asian Earth Sciences* **36**, 459–80.

Isozaki Y, Shimizu N, Yao J, Ji Z and Matsuda T (2007) End-Permian extinction and volcanism-induced environmental stress: Permian–Triassic boundary interval of a lower-slope facies at Chaotian, South China. *Palaeogeography, Palaeoclimatology, Palaeoecology* **252**, 218–38.

Joachimski MM, Lai X, Shen S, Jiang H, Luo G, Chen B, Chen J and Sun Y (2012) Climate warming in the latest Permian and the Permian–Triassic mass extinction. *Geology* **40**, 195–8.

Li GJ, Wang QF, Yu L, Hu ZC, Ma N and Huang YH (2013) Closure time of the Ailaoshan Paleo-Tethys Ocean: Constraints from the zircon U-Pb dating geochemistry of the Late Permian granitoids. *Acta Petrologica Sinica* **29**, 3883–900 (in Chinese with English abstract).

Li SG, Hou ZH, Yang YC, Sun WD, Zhang GW and Li QL (2004) Timing and geochemistry characters of the Sanchazi magmatic arc in Mianlüe tectonic zone, South Qinling. *Science in China (Series D)* **47**, 317–28.

Liao Z, Hu W, Cao J, Wang X, Yao S and Wan Y (2016a) Permian–Triassic boundary (PTB) in the Lower Yangtze Region, southeastern China: a new discovery of deep-water archive based on organic carbon isotopic and U–Pb geochronological studies. *Palaeogeography, Palaeoclimatology, Palaeoecology* **451**, 124–39.

Liao Z, Hu W, Wang X, Cao J, Yao S and Wan Y (2016b) Volcanic origin of claystone near the Permian-Triassic boundary in the deep water environment of the Lower Yangtze region and its implications for LPME. *Acta Geologica Sinica* **90**, 785–800 (in Chinese with English abstract).

Liu FL and Liou JG (2011) Zircon as the best mineral for P–T–time history of UHP metamorphism: a review on mineral inclusions and U-Pb SHRIMP ages of zircons from the Dabie-Sulu UHP rocks. *Journal of Asian Earth Sciences* **40**, 1–39.

https://doi.org/10.1017/S001675681900133X Published online by Cambridge University Press

Liu HC, Wang YJ, Cawood PA, Fan WM, Cai YF and Xing XW (2015) Record of Tethyan ocean closure and Indosinian collision along the Ailaoshan suture zone (SW China). *Gondwana Research* **27**, 1292–306.

Liu HC, Wang YJ, Li ZH, Zi JW and Huangfu PP (2018) Geodynamics of the Indosinian orogeny between the South China and Indochina blocks: insights from latest Permian–Triassic granitoids and numerical modeling. *Geological Society of America Bulletin* **130**, 1289–306.

Liu XC, Jahn BM, Dong SW, Lou YX and Cui JJ (2008) High-pressure metamorphic rocks from Tongbaishan, central China: U-Pb and $^{40}Ar/^{39}Ar$ age constraints on the provenance of protoliths and timing of metamorphism. *Lithos* **105**, 301–18.

Liu XC, Wu YB, Gao S, Wang J, Peng M, Gong HJ, Liu YS and Yuan HL (2011) Zircon U-Pb and Hf evidence for coupled subduction of oceanic and continental crust during the Carboniferous in the Huwan shear zone, western Dabie orogen, central China. *Journal of Metamorphic Geology* **29**, 233–49.

Ludwig KR (2012) *Isoplot 3.75: A Geochronological Toolkit for Microsoft Excel. Berkeley Geochronology Centre, Berkeley, Special Publication no.* **5**, 75 pp.

Meng E, Liu FL, Liu PH, Liu CH, Yang H, Wang F, Shi JR and Cai J (2014) Petrogenesis and tectonic significance of Paleoproterozoic meta-mafic rocks from central Liaodong Peninsula, northeast China: Evidence from zircon U–Pb dating and in situ Lu–Hf isotopes, and whole-rock geochemistry. *Precambrian Research* **247**, 92–109.

Metcalfe I (1996) Pre-Cretaceous evolution of SE Asian terranes. In *Tectonic Evolution of Southeast Asia* (eds R Hall and D Blundell), pp. 97–122. Geological Society of London, Special Publication no. 106.

Metcalfe I (2009) Late Palaeozoic and Mesozoic tectonic and palaeogeographical evolution of SE Asia. In *Late Palaeozoic and Mesozoic Ecosystems in SE Asia* (eds E Buffetaut, G Cuny, J Le Loeuff and V Suteethorn), pp. 7–23. Geological Society of London, Special Publication no. 315.

Metcalfe I (2013) Gondwana dispersion and Asian accretion: Tectonic and palaeogeographic evolution of eastern Tethys. *Journal of Asian Earth Sciences* **66**, 1–33.

Murphy BJ and Nance D (2008) The Pangea conundrum. *Geology* **36**, 703–6.

Ren HD, Wang T, Zhang L, Wang XX, Huang H, Feng CY, Teschner C and Song P (2016) Age, sources and tectonic setting of the Triassic igneous rocks in the easternmost segment of the East Kunlun Orogen, Central China. *Acta Geologica Sinica (English Edition)* **90**, 641–68.

Retallack GJ (2013) Permian and Triassic greenhouse crises. *Gondwana Research* **24**, 90–103.

Retallack GJ and Jahren AH (2008) Methane release from igneous intrusion of coal at the Permian–Triassic boundary. *Journal of Geology* **116**, 1–20.

Rubatto D (2002) Zircon trace element geochemistry: partitioning with garnet and the link between U-Pb ages and metamorphism. *Chemical Geology* **184**, 123–38.

Scotese CR (2004) A continental drift flipbook. *The Journal of Geology* **112**, 729–41.

Scotese CR and McKerrow WS (1990) Revised world maps and introduction. In *Palaeozoic Palaeogeography and Biogeography* (eds WS McKerrow and CR Scotese), pp. 1–21. Geological Society of London, Memoir no. 12.

Shellnutt JG, Wang CY, Zhou MF and Yang Y (2009) Zircon Lu-Hf isotopic compositions of metaluminous and peralkaline A-type granitic plutons of the Emeishan large igneous provence (SW China): constraints on the mantle plume. *Journal of Asian Earth Sciences* **35**, 45–55.

Shen J, Algeo TJ, Feng QL, Zhou L, Feng LP, Zhang N and Huang JH (2013) Volcanically induced environmental change at the Permian–Triassic boundary (Xiakou, Hubei Province, South China): related to West Siberian coalfield methane releases? *Journal of Asian Earth Sciences* **75**, 95–109.

Shen J, Algeo TJ, Hu Q, Zhang N, Zhou L, Xia WC, Xie SC and Feng QL (2012) Negative C-isotope excursions at the Permian–Triassic boundary linked to volcanism. *Geology* **40**, 963–66.

Shen J, Feng Q, Algeo TJ, Li C, Planavsky NJ, Zhou L and Zhang M (2016) Two pulses of oceanic environmental disturbance during the Permian–Triassic boundary crisis. *Earth and Planetary Science Letters* **443**, 139–52.

Shen SZ, Crowley JL, Wang Y, Bowring SA, Erwin DH, Sadler PM, Cao CQ, Rothman DH, Henderson CM, Ramezani J, Zhang H, Shen Y, Wang XD, Wang W, Mu L, Li WZ, Tang YG, Liu XL, Liu LJ, Zeng Y, Jiang YF and Jin YG (2011a) Calibrating the end-Permian mass extinction. *Science* **334**, 1367–72.

Shen WJ, Sun YG, Lin YT, Liu DT and Chai PX (2011b) Evidence for wildfire in the Meishan section and implications for Permian–Triassic events. *Geochimica et Cosmochimica Acta* **75**, 1992–2006.

Shnukov SE, Andreev AV and Savenok SP (1997) Admixture elements in zircons and apatite: a tool for provenances studies of terrigenous sedimentary rocks. In *Proceedings of the Ninth European Union of Geosciences Meeting (EUG 9)*, 23–23 March 1997, Strasbourg, Abstract 65/4P 16:597.

Smith AG and Livermore RA (1991) Pangea in Permian to Jurassic time. *Tectonophysics* **187**, 135–79.

Spörli B, Aita Y, Hori RS and Takemura A (2007) Results of multidisciplinary studies of the Permian/Triassic ocean floor sequence (Waipapa Terrane) at Arrow Rocks in the framework of paleomagnetism in Pre-Neogene rocks from New Zealand. In *The Oceanic Permian/Triassic Boundary Sequence at Arrow Rocks (Oruatemanu), Northland* (eds B Spörli, A Takemura and RS Hori), pp. 219–229. New Zealand: GNS Science Monograph, no. 24.

Stampfli GM, Hochard C, Vérard C, Wilhem C and von Raumer J (2013) The formation of Pangea. *Tectonophysics* **593**, 1–19.

Sun WD, Williams IS and Li SG (2002) Carboniferous and Triassic eclogites in the western Dabie Mountains, east-central China: evidence for protracted convergence of the North and South China Blocks. *Journal of Metamorphic Geology* **20**, 873–86.

Sun YD, Joachimski MM, Wignall PB, Yan CB, Chen YL, Jiang HS, Wang LN and Lai XL (2012) Lethally hot temperatures during the early Triassic greenhouse. *Science* **388**, 366–70.

Svensen H, Planke S, Polozov AG, Schmidbauer N, Corfu F, Podladchikov YY and Jamtveit B (2009) Siberian gas venting and the end-Permian environmental crisis. *Earth and Planetary Science Letters* **277**, 490–500.

Taylor SR and McLennan SM (1981) The composition and evolution of the continental crust—rare-earth element evidence from sedimentary-rocks. *Philosophical Transactions of the Royal Society of London Series A – Mathematical Physical and Engineering Sciences* **301**, 381–99.

van der Meer DG, Spakman W, van Hinsbergen DJJ, Amaru ML and Torsvik TH (2010) Towards absolute plate motions constrained by lower-mantle slab remnants. *Nature Geoscience* **3**, 36–40.

Wang XX, Wang T and Zhang CL (2015) Granitoid magmatism in the Qinling orogen, central China and its bearing on orogenic evolution. *Science China: Earth Sciences* **58**, 1497–512.

Wignall PB (2001) Large igneous provinces and mass extinctions. *Earth-Science Reviews* **53**, 1–33.

Wu FY, Yang YH and Xie LW (2006) Hf isotopic compositions of standard zircons and baddeleyites used in U–Pb geochronology. *Chemical Geology* **231**, 105–26.

Wu YB, Hanchar JM, Gao S, Sylvester PJ, Tubrett M, Qiu HN, Wijbrans JR, Brouwer FM, Yang SH, Yang QJ, Liu YS and Yuan HL (2009) Age and nature of eclogites in the Huwan shear zone, and the multi-stage evolution of the Qinling-Dabie-Sulu orogen, central China. *Earth and Planetary Science Letters* **277**, 345–54.

Xiao WJ, Windley BF, Hao J and Li JL (2002) Arc-ophiolite obduction in the Western Kunlun Range (China): implications for the Palaeozoic evolution of central Asia. *Journal of the Geological Society of London* **159**, 517–28.

Xu L, Lin Y, Shen W, Qi L, Xie L and Ouyang Z (2007) Platinum-group elements of the Meishan Permian–Triassic boundary section: evidence for flood basaltic volcanism. *Chemical Geology* **246**, 55–64.

Xu YG, Luo ZY, Huang XL, He B, Xiao L, Xie LW and Shi YR (2008) Zircon U–Pb and Hf isotope constraints on crustal melting associated with the Emeishan mantle plume. *Geochimica et Cosmochimica Acta* **72**, 3084–104.

Yan Z, Bian QT, Korchagin OA, Pospelov II, Li JL and Wang ZQ (2008) Provenance of Early Triassic Hongshuichuan Formation in the southern margin of the East Kunlun Mountains: Constrains from detrital framework, heavy mineral analysis and geochemistry. *Acta Petrologica Sinica* **24**, 1068–78 (in Chinese with English abstract).

Yan Z, Guo X, Fu C, Aitchison J, Wang Z and Li J (2014) Detrital heavy mineral constraints on the Triassic tectonic evolution of the West Qinling terrane, NW China: Implications for understanding subduction of the Paleotethyan Ocean. *The Journal of Geology* **122**, 591–608.

https://doi.org/10.1017/S001675681900133X Published online by Cambridge University Press

Yan Z, Wang ZQ, Li JL, Xu ZQ and Deng JF (2012) Tectonic settings and accretionary orogenesis of the West Qinling Terrane, northeastern margin of the Tibet Plateau. *Acta Petrologica Sinica* **28**, 1808–28 (in Chinese with English abstract).

Yang JH, Cawood PA, Du YS, Huang H, Huang HW and Tao P (2012) Large Igneous Province and magmatic arc sourced Permian–Triassic volcanogenic sediments in China. *Sedimentary Geology* **261**, 120–31.

Yang ZY, Ma XH, Huang BC, Sun ZM and Zhou YX (1998) Apparent polar wander path and tectonic movement of the North China Block in Phanerozoic. *Science in China (Series D)* **41**, 51–65.

Yang ZY, Wu SB, Yin HF, Xu GR, Zhang KX and Bi XM (1991) *Geological Events of Permo-Triassic Transitional Period in South China*. Beijing: Geological Publishing House, 190 pp. (in Chinese with English abstract).

Yin HF, Feng QL, Lai XL, Baud A and Tong JN (2007) The protracted Permo-Triassic crisis and multi-episode extinction around the Permian–Triassic boundary. *Global and Planetary Change* **55**, 1–20.

Yin HF, Huang SJ, Zhang KX, Hansen HJ, Yang FQ, Ding MH and Bie X (1992) The effects of volcanism on the Permo-Triassic mass extinction in South China. In *Permo-Triassic events in the eastern Tethys: stratigraphy, classification, and relations with the Western Tethys* (eds WC Sweet, ZY Yang, JM Dickins and HF Yin), pp. 146–57. Cambridge: Cambridge University Press.

Yin HF, Huang SJ, Zhang KX, Yang FQ, Ding MH, Bi XM and Zhang SX (1989) Volcanism at the Permian–Triassic boundary in South China and its effects on mass extinction. *Acta Geologica Sinica (English Edition)* **62**, 169–81.

Zhang G, Dong Y, Lai S, Guo A, Meng Q, Liu S, Cheng S, Yao A, Zhang Z, Pei X and Li S (2004) Mianlue tectonic zone and Mianlue suture zone on southern margin of Qinling–Dabie orogenic belt. *Science in China (Series D)* **47**, 300–16.

Zhang ZY, He WH, Zhang Y, Yang TL and Wu SB (2009) Late Permian–earliest Triassic ammonoid sequences from the Rencunping section, Sangzhi County, Hunan Province, South China and their regional correlation. *Geological Science and Technology Information* **28**, 23–30 (in Chinese with English abstract).

Zhao GC, Zhang GW, Wang YJ, Huang BC, Dong YP, Li SZ and Yu S (2018) Geological reconstructions of the East Asian blocks: from the breakup of Rodinia to the assembly of Pangea. *Earth-Science Reviews* **186**, 262–86.

Zhao XX and Coe RS (1987) Palaeomagnetic constraints on the collision and rotation of North and South China. *Nature* **327**, 141–4.

Zheng B, Mou C, Wang X, Xiao Z and Chen Y (2019) Sedimentary record of the collision of the North and South China cratons: new insights from the Western Hubei Trough. *Geological Journal* 54(6), 3335–48.

Zhong H, Campbell IH, Zhu WG, Allen CM, Hu RZ, Xie LW and He DF (2011) Timing and source constraints on the relationship between mafic and silicic intrusions in the Emeishan large igneous province. *Geochimica et Cosmochimica Acta* **75**, 1374–95.

Zhong H, Zhu WG, Hu RZ, Xie LW, He DF, Liu F and Chu ZY (2009) Zircon U–Pb age and Sr–Nd–Hf isotope geochemistry of the Panzhihua A-type syenitic intrusion in the Emeishan large igneous province, southwest China and implications for growth of juvenile crust. *Lithos* **110**, 109–28.

Zhu J, Zhang ZC, Hou T and Kang JL (2011) LA-ICP-MS zircon U-Pb geochronology of the tuffs on the uppermost of the Emeishan basalt succession in Panxian County, Guizhou Province: Constraints on genetic link between Emeishan large igneous province and the mass extinction. *Acta Petrologica Sinica* **27**, 2743–51 (in Chinese with English abstract).

Zhu RX, Yang ZY, Wu HN, Ma XH, Huang BC, Meng ZF and Fang DJ (1998) Paleomagnetic constraints on the tectonic history of the major blocks of China during the Phanerozoic. *Science in China (Series D)* **41**, 1–19.

Zi JW, Cawood PA, Fan WM, Tohver E, Wang YJ and McCuaig TC (2012) Generation of early Indosinian enriched mantle-derived granitoid pluton in the Sanjiang Orogen (SW China) in response to closure of the Paleo-Tethys. *Lithos* **140–141**, 166–82.

https://doi.org/10.1017/S001675681900133X Published online by Cambridge University Press